

Searching for ultra- and hyper- luminous X-ray sources in the *Swift-XRT* catalog

Supervisor: Dr. Olivier GODET
April-September 2020

Clément Pellouin

M2 Internship Presentation IRAP

September 30th, 2020

Contents

1 Introduction

- Formation paths of Supermassive Black Holes (SMBHs)
- ULXs & HLXs
- Data mining in multi-wavelength catalogs

2 ULX/HLX candidates selection

- The ULX/HLX sample
- ULX/HLX sample cleaning

3 HLX candidate in NGC 5917

- X-ray data analysis
- MUSE data analysis

4 Conclusion

Introduction
●oooooooooooo

ULX/HLX candidates selection
oooooooooooo

HLX candidate in NGC 5917
oooooooooooooooooooooooooooo

Conclusion
oooooo

Backup
oooooooooooooooooooo

Introduction

How to grow an SMBH?

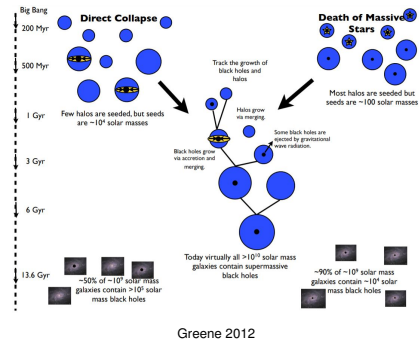
Observations

- $8 \times 10^8 M_{\odot}$ SMBH at $z = 7.5$ Banados et al. 2018
- $2 \times 10^9 M_{\odot}$ SMBH in a quasar at $z = 7.1$ Mortlock et al. 2011
- Masses up to $6.6 \times 10^{10} M_{\odot}$ Shemmer et al. 2004

SMBH growth scenarios

- Hierarchical growth by successive intermediate-mass BH mergers Farouki et al 1983

$$100 M_{\odot} \lesssim M_{IMBH} \lesssim 10^5 M_{\odot}$$
 Miller & Colbert 2004
- Sustained accretion episodes at high accretion rates



ULXs & HLXs

Definition Feng et al 2011

- Extragalactic off-nuclear X-ray source powered by accretion of matter
- ULX: Isotropic equivalent $L_X \geq 10^{39} \text{ erg} \cdot \text{s}^{-1}$ (0.3 – 10 keV)
- HLX: Isotropic equivalent $L_X \geq 10^{41} \text{ erg} \cdot \text{s}^{-1}$ (0.3 – 10 keV)

ULXs: super-Eddington accretion?

- bubbles observed around some ULXs (winds/radiation) Pakull & Mirioni 2002
- 6 persisting pulsating ULXs discovered with period spin-up Bachetti et al 2014: NS progenitors ($\sim 1.4 - 1.5 M_{\odot}$) with strongly super-Eddington accretion ($L_X \gg 10^{38} \text{ erg} \cdot \text{s}^{-1}$)

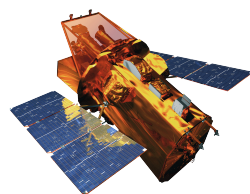
HLXs: accreting IMBHs?

- Very few candidates:
- HLX-1 Farrell et al 2009 has multi-wavelength properties similar to an X-ray binary (XRB), but 1000 times more luminous
- Tidal Disruption Event (TDE) Lin et al 2018

The Neil Gehrels *Swift* observatory

Characteristics Gehrels et al. 2004

- Multi-wavelength gamma-ray burst (GRB) observatory
- Carries 3 instruments:
 - BAT (Burst Alert Telescope, Barthelmy et al. 2005): GRB prompt emission detection at 15 – 150 keV
 - XRT (X-ray Telescope, Burrows et al. 2005): sky observation at 0.3 – 10 keV (GRB afterglows, X-ray source monitoring)
 - UVOT (Ultraviolet/Optical Telescope, Roming et al. 2005): 6 filters for a sensitivity at 160 – 600 nm
- Automatic sky localization and repositioning after a GRB detection



The *Swift* spacecraft model

Credit: NASA E/PO

The 2SXPS catalog

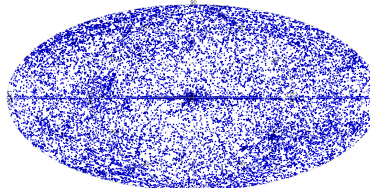
Evans et al 2020

Characteristics

- *Swift-XRT* observations between 2005-01-01 and 2018-08-31
- 206335 X-ray sources
- Sky coverage: 3790 deg²
- Up to 230 data columns per source (Position, Exposure, Flags, Count rates, Spectral/Flux information, Cross-correlations)

Assets

- High number of unknown sources (~ 90 % not observed by *XMM-Newton*)
- Large sky coverage
- Simultaneous UVOT observations
- Short- and long-term monitoring of sources (from ~ 1 s to ~ 10 years)
- Online tools available



Positions of the sources of 2SXPS in the Galactic coordinates

Introduction
oooooooooooo

ULX/HLX candidates selection
●oooooooooooo

HLX candidate in NGC 5917
oooooooooooooooooooooooooooo

Conclusion
oooooo

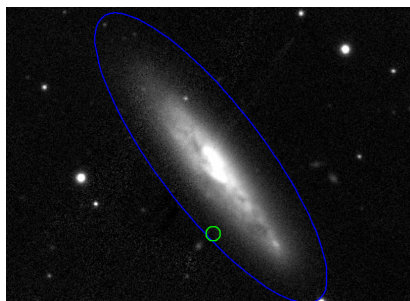
Backup
oooooooooooooooooooo

ULX/HLX candidates selection

Producing a ULX/HLX sample

Table Brouwer for 31 matches at GLADE 3.0 P1

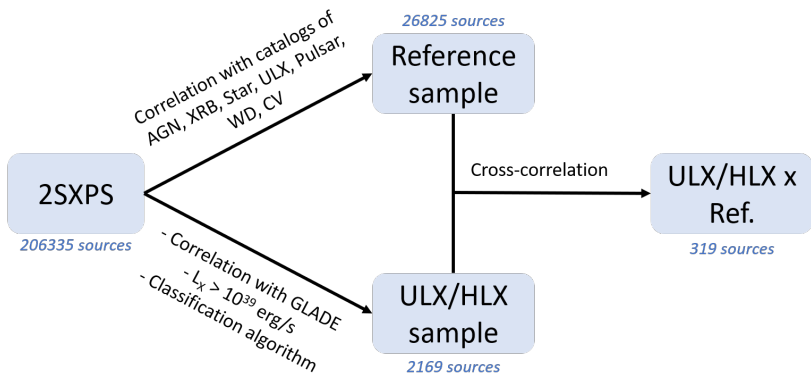
Name	lat	lon	Hert	BH	Ra (J2000)	Dec (J2000)	Ext	Mflux	EM-DM	MM-DM	PA	ref	PCF_PDF	Grained	
NGC 5917	-1.245	2.922			12h 51m 40s	+21° 04' 29"	9.5	188.0	169.74	16. 739	-0. 633	421. 2	1	GLADE	85529
IC 10	-1.192	1.019			10h 42m 37s	-23° 00' 28"	-2.1	169.48	167.50	15. 688	-0. 490	353. 2	1	GLADE	85530
NGC 5917	-1.245	2.922			12h 51m 40s	+21° 04' 29"	9.5	188.0	169.74	16. 739	-0. 633	421. 2	1	GLADE	85531
NGC 5917	-1.245	2.922			12h 51m 40s	+21° 04' 29"	9.5	188.0	169.74	16. 739	-0. 633	421. 2	1	GLADE	85532
NGC 5917	-1.245	2.922			12h 51m 40s	+21° 04' 29"	9.5	188.0	169.74	16. 739	-0. 633	421. 2	1	GLADE	85533
NGC 5917	-1.245	2.922			12h 51m 40s	+21° 04' 29"	9.5	188.0	169.74	16. 739	-0. 633	421. 2	1	GLADE	85534
NGC 5917	-1.245	2.922			12h 51m 40s	+21° 04' 29"	9.5	188.0	169.74	16. 739	-0. 633	421. 2	1	GLADE	85535
NGC 5917	-1.245	2.922			12h 51m 40s	+21° 04' 29"	9.5	188.0	169.74	16. 739	-0. 633	421. 2	1	GLADE	85536
NGC 5917	-1.245	2.922			12h 51m 40s	+21° 04' 29"	9.5	188.0	169.74	16. 739	-0. 633	421. 2	1	GLADE	85537
NGC 5917	-1.245	2.922			12h 51m 40s	+21° 04' 29"	9.5	188.0	169.74	16. 739	-0. 633	421. 2	1	GLADE	85538
NGC 5917	-1.245	2.922			12h 51m 40s	+21° 04' 29"	9.5	188.0	169.74	16. 739	-0. 633	421. 2	1	GLADE	85539
NGC 5917	-1.245	2.922			12h 51m 40s	+21° 04' 29"	9.5	188.0	169.74	16. 739	-0. 633	421. 2	1	GLADE	85540
NGC 5917	-1.245	2.922			12h 51m 40s	+21° 04' 29"	9.5	188.0	169.74	16. 739	-0. 633	421. 2	1	GLADE	85541
NGC 5917	-1.245	2.922			12h 51m 40s	+21° 04' 29"	9.5	188.0	169.74	16. 739	-0. 633	421. 2	1	GLADE	85542
NGC 5917	-1.245	2.922			12h 51m 40s	+21° 04' 29"	9.5	188.0	169.74	16. 739	-0. 633	421. 2	1	GLADE	85543
NGC 5917	-1.245	2.922			12h 51m 40s	+21° 04' 29"	9.5	188.0	169.74	16. 739	-0. 633	421. 2	1	GLADE	85544
NGC 5917	-1.245	2.922			12h 51m 40s	+21° 04' 29"	9.5	188.0	169.74	16. 739	-0. 633	421. 2	1	GLADE	85545
NGC 5917	-1.245	2.922			12h 51m 40s	+21° 04' 29"	9.5	188.0	169.74	16. 739	-0. 633	421. 2	1	GLADE	85546
NGC 5917	-1.245	2.922			12h 51m 40s	+21° 04' 29"	9.5	188.0	169.74	16. 739	-0. 633	421. 2	1	GLADE	85547
NGC 5917	-1.245	2.922			12h 51m 40s	+21° 04' 29"	9.5	188.0	169.74	16. 739	-0. 633	421. 2	1	GLADE	85548
NGC 5917	-1.245	2.922			12h 51m 40s	+21° 04' 29"	9.5	188.0	169.74	16. 739	-0. 633	421. 2	1	GLADE	85549
NGC 5917	-1.245	2.922			12h 51m 40s	+21° 04' 29"	9.5	188.0	169.74	16. 739	-0. 633	421. 2	1	GLADE	85550
NGC 5917	-1.245	2.922			12h 51m 40s	+21° 04' 29"	9.5	188.0	169.74	16. 739	-0. 633	421. 2	1	GLADE	85551
NGC 5917	-1.245	2.922			12h 51m 40s	+21° 04' 29"	9.5	188.0	169.74	16. 739	-0. 633	421. 2	1	GLADE	85552
NGC 5917	-1.245	2.922			12h 51m 40s	+21° 04' 29"	9.5	188.0	169.74	16. 739	-0. 633	421. 2	1	GLADE	85553
NGC 5917	-1.245	2.922			12h 51m 40s	+21° 04' 29"	9.5	188.0	169.74	16. 739	-0. 633	421. 2	1	GLADE	85554
NGC 5917	-1.245	2.922			12h 51m 40s	+21° 04' 29"	9.5	188.0	169.74	16. 739	-0. 633	421. 2	1	GLADE	85555
NGC 5917	-1.245	2.922			12h 51m 40s	+21° 04' 29"	9.5	188.0	169.74	16. 739	-0. 633	421. 2	1	GLADE	85556
NGC 5917	-1.245	2.922			12h 51m 40s	+21° 04' 29"	9.5	188.0	169.74	16. 739	-0. 633	421. 2	1	GLADE	85557
NGC 5917	-1.245	2.922			12h 51m 40s	+21° 04' 29"	9.5	188.0	169.74	16. 739	-0. 633	421. 2	1	GLADE	85558
NGC 5917	-1.245	2.922			12h 51m 40s	+21° 04' 29"	9.5	188.0	169.74	16. 739	-0. 633	421. 2	1	GLADE	85559
NGC 5917	-1.245	2.922			12h 51m 40s	+21° 04' 29"	9.5	188.0	169.74	16. 739	-0. 633	421. 2	1	GLADE	85560
NGC 5917	-1.245	2.922			12h 51m 40s	+21° 04' 29"	9.5	188.0	169.74	16. 739	-0. 633	421. 2	1	GLADE	85561
NGC 5917	-1.245	2.922			12h 51m 40s	+21° 04' 29"	9.5	188.0	169.74	16. 739	-0. 633	421. 2	1	GLADE	85562
NGC 5917	-1.245	2.922			12h 51m 40s	+21° 04' 29"	9.5	188.0	169.74	16. 739	-0. 633	421. 2	1	GLADE	85563
NGC 5917	-1.245	2.922			12h 51m 40s	+21° 04' 29"	9.5	188.0	169.74	16. 739	-0. 633	421. 2	1	GLADE	85564
NGC 5917	-1.245	2.922			12h 51m 40s	+21° 04' 29"	9.5	188.0	169.74	16. 739	-0. 633	421. 2	1	GLADE	85565
NGC 5917	-1.245	2.922			12h 51m 40s	+21° 04' 29"	9.5	188.0	169.74	16. 739	-0. 633	421. 2	1	GLADE	85566
NGC 5917	-1.245	2.922			12h 51m 40s	+21° 04' 29"	9.5	188.0	169.74	16. 739	-0. 633	421. 2	1	GLADE	85567
NGC 5917	-1.245	2.922			12h 51m 40s	+21° 04' 29"	9.5	188.0	169.74	16. 739	-0. 633	421. 2	1	GLADE	85568
NGC 5917	-1.245	2.922			12h 51m 40s	+21° 04' 29"	9.5	188.0	169.74	16. 739	-0. 633	421. 2	1	GLADE	85569
NGC 5917	-1.245	2.922			12h 51m 40s	+21° 04' 29"	9.5	188.0	169.74	16. 739	-0. 633	421. 2	1	GLADE	85570
NGC 5917	-1.245	2.922			12h 51m 40s	+21° 04' 29"	9.5	188.0	169.74	16. 739	-0. 633	421. 2	1	GLADE	85571
NGC 5917	-1.245	2.922			12h 51m 40s	+21° 04' 29"	9.5	188.0	169.74	16. 739	-0. 633	421. 2	1	GLADE	85572
NGC 5917	-1.245	2.922			12h 51m 40s	+21° 04' 29"	9.5	188.0	169.74	16. 739	-0. 633	421. 2	1	GLADE	85573
NGC 5917	-1.245	2.922			12h 51m 40s	+21° 04' 29"	9.5	188.0	169.74	16. 739	-0. 633	421. 2	1	GLADE	85574
NGC 5917	-1.245	2.922			12h 51m 40s	+21° 04' 29"	9.5	188.0	169.74	16. 739	-0. 633	421. 2	1	GLADE	85575
NGC 5917	-1.245	2.922			12h 51m 40s	+21° 04' 29"	9.5	188.0	169.74	16. 739	-0. 633	421. 2	1	GLADE	85576
NGC 5917	-1.245	2.922			12h 51m 40s	+21° 04' 29"	9.5	188.0	169.74	16. 739	-0. 633	421. 2	1	GLADE	85577
NGC 5917	-1.245	2.922			12h 51m 40s	+21° 04' 29"	9.5	188.0	169.74	16. 739	-0. 633	421. 2	1	GLADE	85578
NGC 5917	-1.245	2.922			12h 51m 40s	+21° 04' 29"	9.5	188.0	169.74	16. 739	-0. 633	421. 2	1	GLADE	85579
NGC 5917	-1.245	2.922			12h 51m 40s	+21° 04' 29"	9.5	188.0	169.74	16. 739	-0. 633	421. 2	1	GLADE	85580
NGC 5917	-1.245	2.922			12h 51m 40s	+21° 04' 29"	9.5	188.0	169.74	16. 739	-0. 633	421. 2	1	GLADE	85581
NGC 5917	-1.245	2.922			12h 51m 40s	+21° 04' 29"	9.5	188.0	169.74	16. 739	-0. 633	421. 2	1	GLADE	85582
NGC 5917	-1.245	2.922			12h 51m 40s	+21° 04' 29"	9.5	188.0	169.74	16. 739	-0. 633	421. 2	1	GLADE	85583
NGC 5917	-1.245	2.922			12h 51m 40s	+21° 04' 29"	9.5	188.0	169.74	16. 739	-0. 633	421. 2	1	GLADE	85584
NGC 5917	-1.245	2.922			12h 51m 40s	+21° 04' 29"	9.5	188.0	169.74	16. 739	-0. 633	421. 2	1	GLADE	85585
NGC 5917	-1.245	2.922			12h 51m 40s	+21° 04' 29"	9.5	188.0	169.74	16. 739	-0. 633	421. 2	1	GLADE	85586
NGC 5917	-1.245	2.922			12h 51m 40s	+21° 04' 29"	9.5	188.0	169.74	16. 739	-0. 633	421. 2	1	GLADE	85587
NGC 5917	-1.245	2.922			12h 51m 40s	+21° 04' 29"	9.5	188.0	169.74	16. 739	-0. 633	421. 2	1	GLADE	85588
NGC 5917	-1.245	2.922			12h 51m 40s	+21° 04' 29"	9.5	188.0	169.74	16. 739	-0. 633	421. 2	1	GLADE	85589
NGC 5917	-1.245	2.922			12h 51m 40s	+21° 04' 29"	9.5	188.0	169.74	16. 739	-0. 633	421. 2	1	GLADE	85590



The ULX/HLX sample

- 2169 candidates Godet, Pellouin, Tranin et al, in prep
- Selection process:
 - GLADE association
 - Unabsorbed $L_X \geq 10^{39}$ erg · s⁻¹ (0.3 – 10 keV)
 - Not located in the galactic center
 - Detection flag: Good

Finding reference sources



Classifying the sources of the ULX/HLX sample

Classification algorithm

- Probabilistic classification based on the properties observed in the reference sample
- 2169 sources classified as AGNs (43%), XRBs (52%), Stars (3%), CVs (cataclysmic variables, 1%) Tranin, Pellouin et al, in prep

Using the ULX/HLX sample, two main objectives:

- Cleaning the ULX/HLX sample
- Analyzing the best ULX/HLX candidates

Classification analysis

Analysis of the classes distribution:

Class	Reference		ULX/HLX x Ref.		ULX/HLX (prediction)	
	Count	%	Count	%	Count	%
AGN	20799	77	134	42	943	43
Star	5181	19	19	6	74	3
XRB	475	2	165	52	1138	52
CV	370	1	1	0	14	1

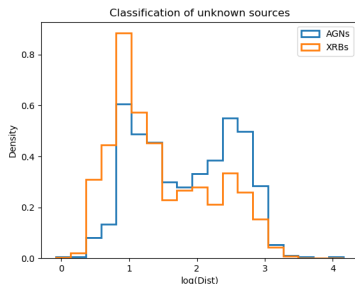
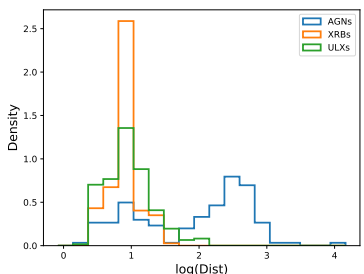
Comparison of statistics on the classes of sources

Conclusions

- ULX/HLX definition non-physical, but many XRBs retrieved in the ULX/HLX sample
- Potentially high level of AGN contamination
- Contaminants are mostly background AGNs instead of foreground stars

ULX/HLX sample cleaning

Classification analysis



Comparison of statistics on the classes of sources

Conclusions

- ULX/HLX definition non-physical, but many XRBs retrieved in the ULX/HLX sample
- Potentially high level of AGN contamination
- Contaminants are mostly background AGNs instead of foreground stars

Classification analysis

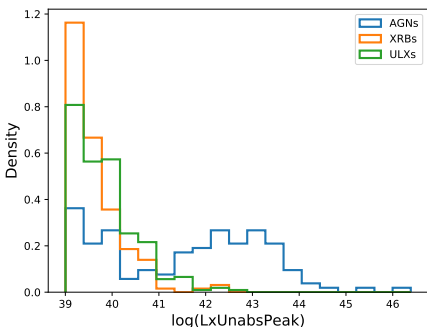
How to select the best ULX/HLX candidates among the 2169 sources?

Prediction	AGN	Star	XRB	CV
Literature				
AGN	132	1	2	0
Star	2	17	0	0
XRB	42	7	84	2
CV	0	0	1	0

Confusion matrix of the classification source types

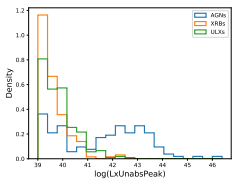
Focusing only on the sources classified as XRBs?

Identification of new selection parameters

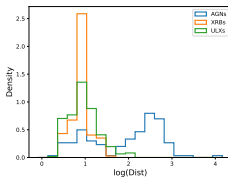


Distribution of the unabsorbed X-ray peak luminosity for the sources of the cross-correlated sample. In blue, sources whose known class is AGN, in yellow, those that are XRBS, in green, sources found in catalogs of ULXs

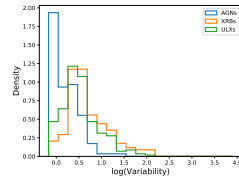
Identification of new selection parameters



Unabsorbed X-ray peak luminosity



Distance



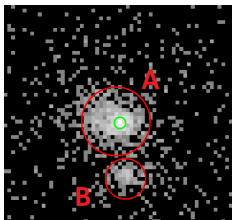
Variability

Objective = Finding interesting sources to study:

- Focus on sources that are in a MUSE cube (400/2169)
- Focus on sources with other multi-wavelength observations
- Focus on sources with *XMM-Newton* and/or *Chandra* observations

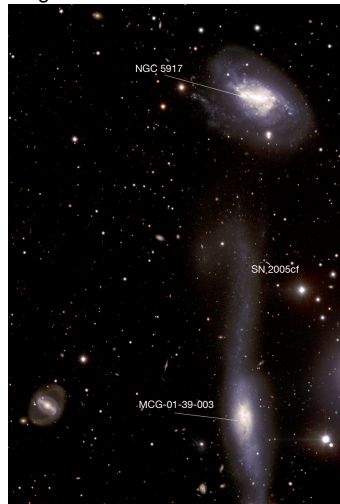
HLX candidate in NGC 5917

2SXPS J152131.9-072242



Swift-XRT image of 2SXPS
J152131.9-072242

VLT image of NGC 5917 and MCG-01-39-003



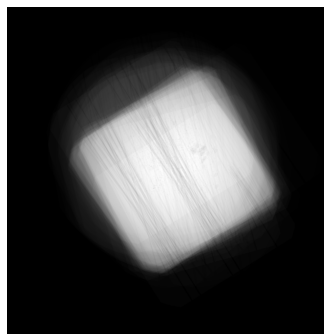
Fact sheet

- RA(J2000): $15^h 21^m 31.99^s$
- Dec(J2000): $-07^\circ 22' 42.4''$
- Associated with NGC 5917, interacting spiral galaxy
- $9''$ (1.3 kpc) away from the galactic center
- $d_{NGC5917} = 30.8 \text{ Mpc}$

Swift-XRT raw data processing

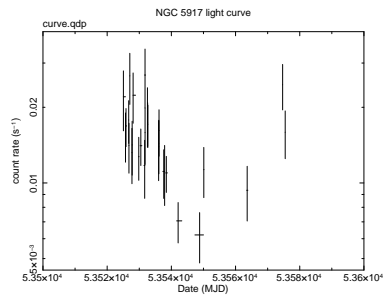
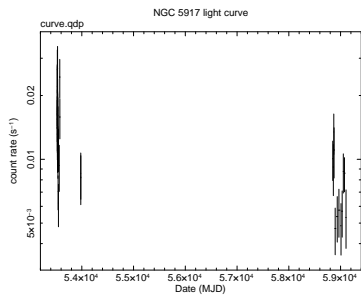
Preprocessing steps, using XSELECT

- Produce a clean, stacked event list (events = photons detections on the CCD)
- Produce an exposure map (dead pixels & columns, vignetting)
- Take into account the CCD temporal and spectral response to incoming photons
- Filter bad events



Exposure map for the *Swift*-XRT observations of NGC 5917

X-ray light curve



Left: Light curve showing the 2 series of observations observations of 2SXPS J152131.9-072242 taken between 2005-06-04 and 2020-08-28, in the 0.3 – 10 keV band. Every bin has a 20-count statistic. **Right:** Zoom on the light curve between 2005-06-04 and 2005-07-23.

MUSE data analysis

MUSE = Integral field Unit (IFU) taking data cubes (300×300 pixels, ~ 3500 -bins visible spectra from 4750 \AA to 9350 \AA) Bacon et al 2010

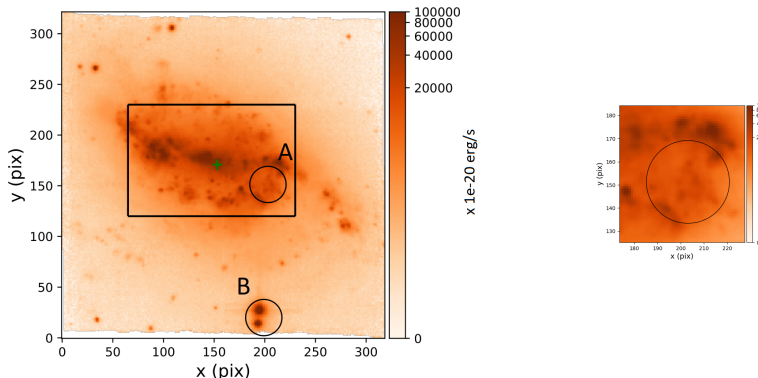
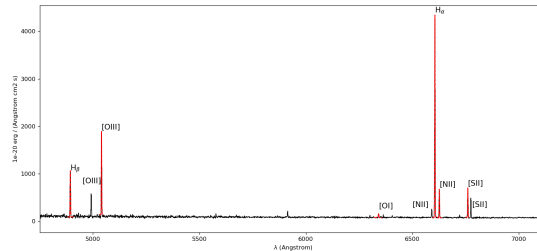


Image of NGC 5917 taken by MUSE on 2016-05-31 in the $6500 \text{ \AA} - 6624 \text{ \AA}$ band (centered on H α).
Intensity in units of $10^{-20} \text{ erg} \cdot \text{s}^{-1} \cdot \text{cm}^{-2}$.
Spatial resolution: $0.5''$

Spectral fitting

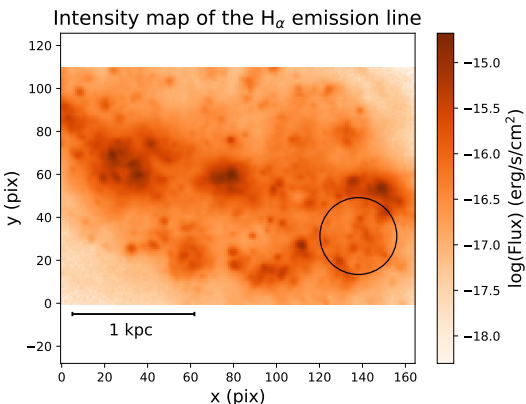
Fitting technique

- Based on the Python library `mpdaf`
- Emission lines fitted by gaussian profiles
- χ^2 minimization
- Output parameters: wavelength of the peak, peak value, FWHM, continuum, integrated flux under the gaussian, 1σ errors on these parameters



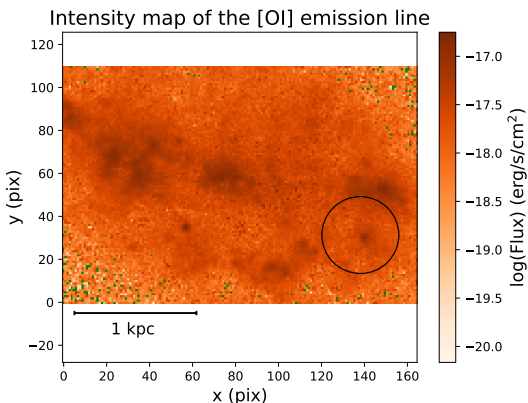
Spectrum of MUSE cube pixel located at the center of the *Swift-XRT* error circle

Spectral ray luminosity maps



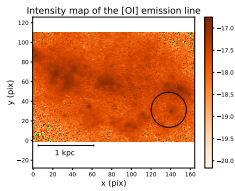
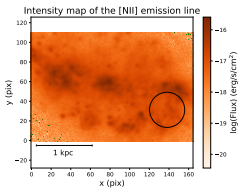
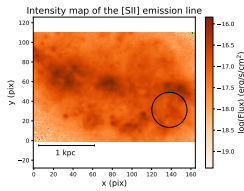
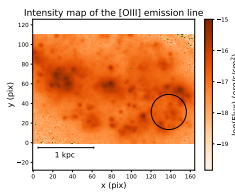
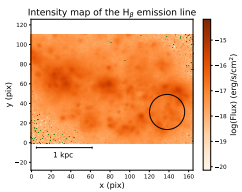
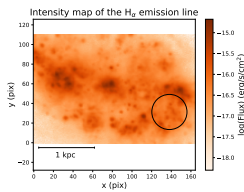
Integrated flux under the fitted gaussian on the H α emission line

Spectral ray luminosity maps



Integrated flux under the fitted gaussian on the [OI] emission line

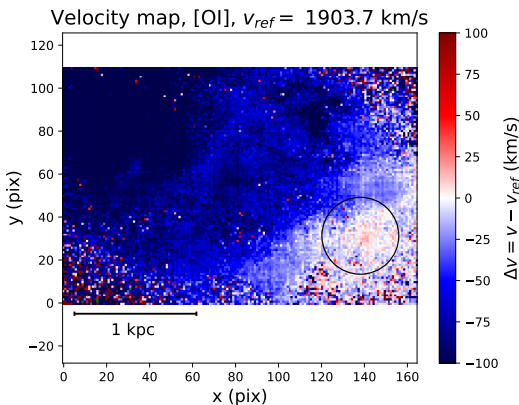
Spectral ray luminosity maps



Top row, left to right: H α , H β , [OIII]. Bottom row: [SII], [NII], [OI]

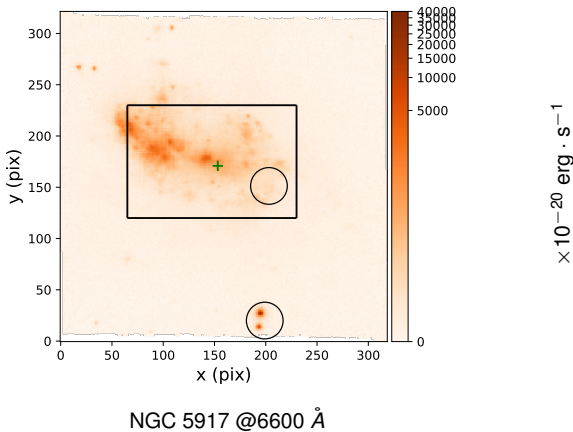
Velocity maps

$$\text{Emission line redshift velocity: } v = c \times \frac{\lambda_{\text{obs}} - \lambda_{\text{ref}}}{\lambda_{\text{ref}}}$$



Velocity map of NGC5917 from the [OI] emission line fitting. Each pixel color represents the relative velocity computed from the gaussian fit of the emission line

MUSE Images around H α



Introduction
○○○○○○○○○○

ULX/HLX candidates selection
○○○○○○○○○○

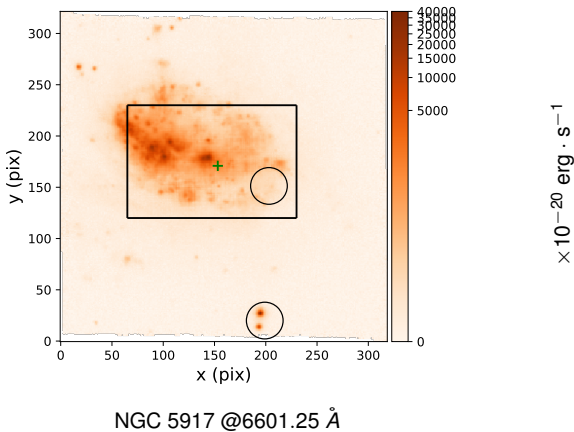
HLX candidate in NGC 5917
○○○○○○○○○○●○○○○○○○○○○

Conclusion
○○○○○

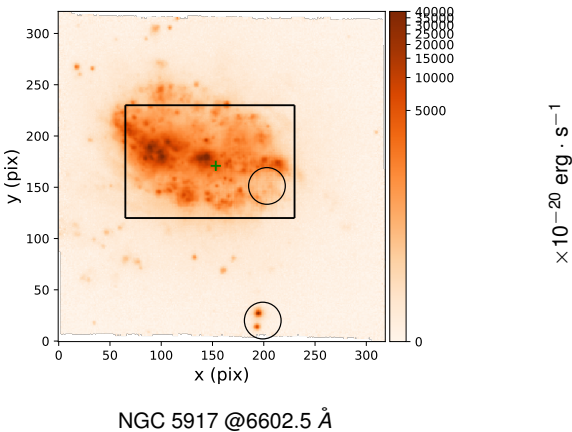
Backup
○○○○○○○○○○○○○○○○

MUSE data analysis

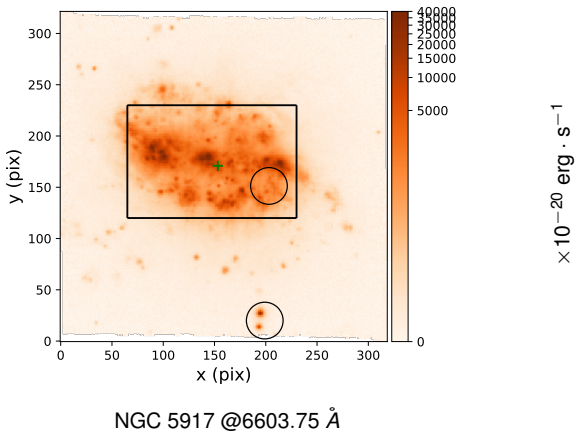
MUSE Images around H α



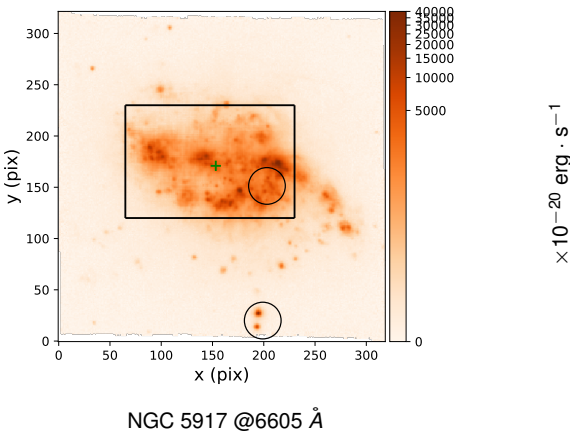
MUSE Images around H α



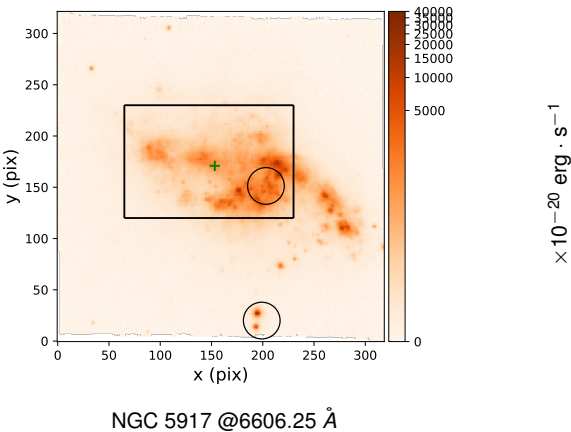
MUSE Images around H α



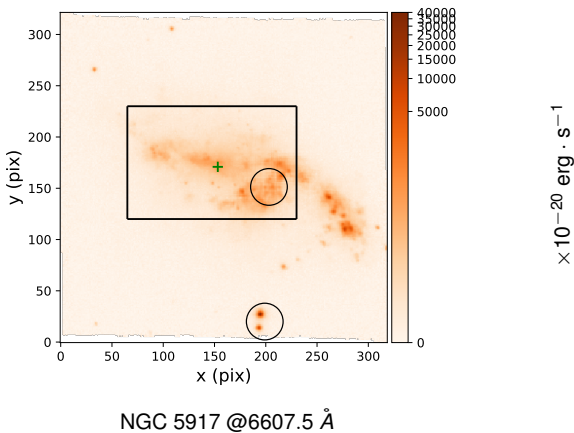
MUSE Images around H α



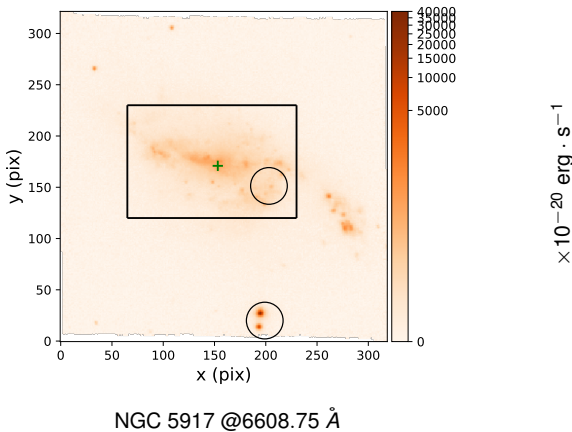
MUSE Images around H α



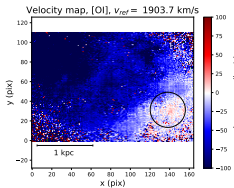
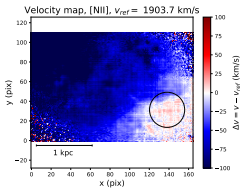
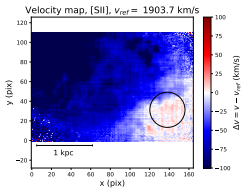
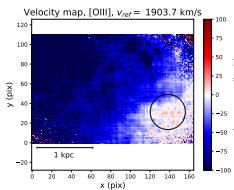
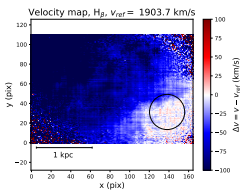
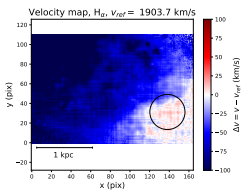
MUSE Images around H α



MUSE Images around H α



Velocity maps



Top row, left to right: H α , H β , [OIII]. Bottom row: [SII], [NII], [OI]

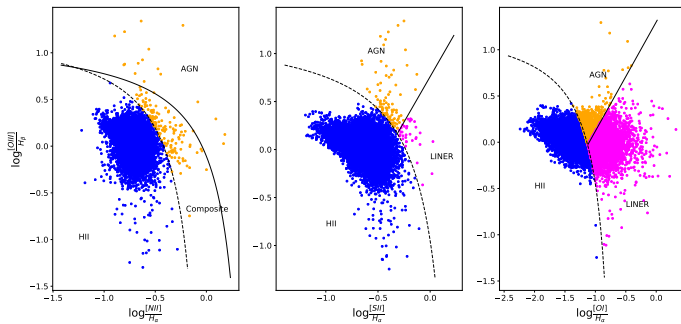
BPT Diagnostic

Characteristics

- Introduced by Baldwin, Phillips and Telervich Baldwin et al. 1981
- Originally proposed to diagnose AGNs, Low-Ionization Nuclear Emission-line Regions (LINER), and HII ionization regions
- Now also used to probe the local gas ionization mechanism:
 - photo-ionization due to UV photons from young, hot stars;
 - photo-ionization from accretion activity;
 - shock ionization
- Uses 3 different line ratios plots:
 - [OIII]/H β versus [NII]/H α
 - [OIII]/H β versus [SII]/H α
 - [OIII]/H β versus [OI]/H α

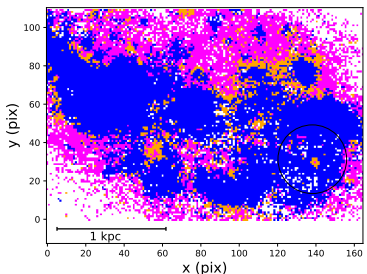
BPT Diagnostic

BPT diagnostic of NGC 5917

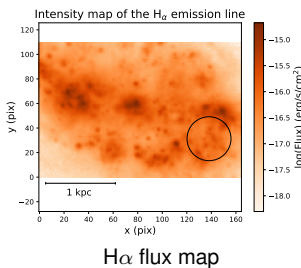


BPT diagnostics for different emission line ratios in NGC 5917

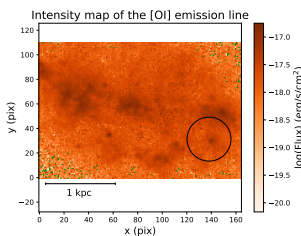
BPT Diagnostic



[OIII]/H β versus [OI]/H α BPT diagnostic map



H α flux map



[OI] flux map

Introduction
oooooooooooo

ULX/HLX candidates selection
oooooooooooo

HLX candidate in NGC 5917
oooooooooooooooooooooooooooo

Conclusion
●ooooo

Backup
oooooooooooooooooooo

Conclusion

Conclusion

- Search for IMBHs and super-Eddington accretion
- X-ray catalogs correlated with multi-wavelength catalogs
- ULX/HLX candidates sample (2169 candidates)
- Tools to clean the sample (1221 candidates)
- Focus on sources with MUSE cubes (400/2169)
- 3 good candidates identified
- Multi-wavelength approach to study them

Analysis of the best candidates

In NGC 5917

- *Swift*-XRT X-ray observations:
 - Average unabsorbed luminosity $L_X = (3.1 \pm 0.3) \times 10^{40} \text{ erg} \cdot \text{s}^{-1}$
 - Flux variation by a factor ~ 4 between 2005 and 2020
- MUSE observations:
 - NGC 5917 rotating as a whole
 - An optical source showed a more intense [OI] line emission
 - BPT diagnostic showed gas ionization due to accretion in this region
- Probable association of the optical counterpart to the X-ray source

Other sources studied

- In NGC 3252
 - Source vanished between 2011 and 2020 (more than 40 times fainter)
 - *Swift*-UVOT counterpart found
- In NGC 3583
 - Source found using my selection method
 - HST observations show structures, likely star-forming, in the region of the source

Perspectives and continuations

Perspectives

- Study of the X-ray luminosity function
- Systematic study of the host galaxies properties (interacting, dwarf, spiral, star-forming, ...)
- Analysis of the reference sample contamination rates
- Determination of the fraction of background sources using MUSE cubes
- Using HST analyses for more sources

Perspectives and continuations

Proposals

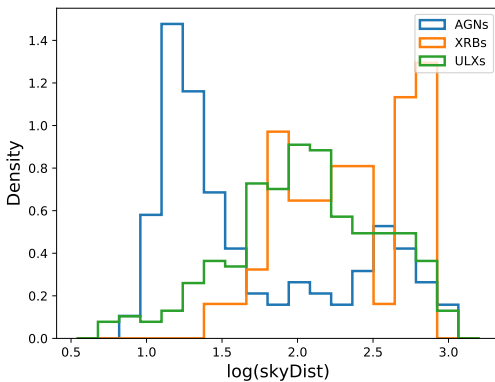
- *XMM-Newton* observation of NGC 3252 at the end of the year
- Possible observation of NGC 5917 and NGC 3583 by *Swift* in 2021-2022 (proposal submitted) and by *XMM-Newton* (proposal in prep Pellouin 2020)

Papers

- Presentation of the ULX/HLX candidates sample Godet, Pellouin, Tranin et al, in prep
- Classification of X-ray sources: an example with 2SXPS Tranin, ..., Pellouin et al, in prep.
- NGC 5917 HLX candidate discovery Pellouin et al, in prep.
- NGC 3252 analysis following *XMM-Newton* observations Tranin et al, in prep.
- NGC 3583 HLX candidate discovery Pellouin et al, in prep.

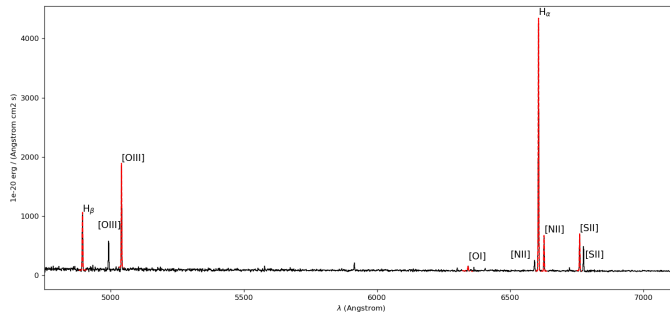
Thanks!

Spectral fitting



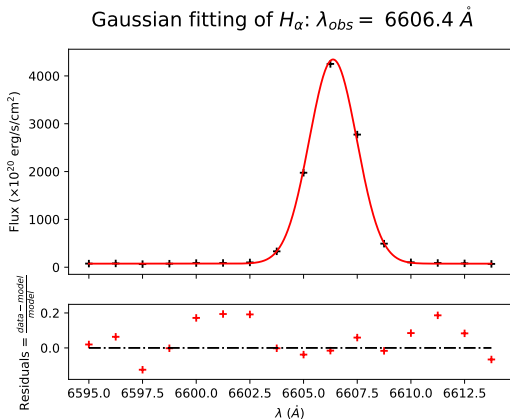
Distribution of the distances to the galactic center (in arcsec)

Spectral fitting



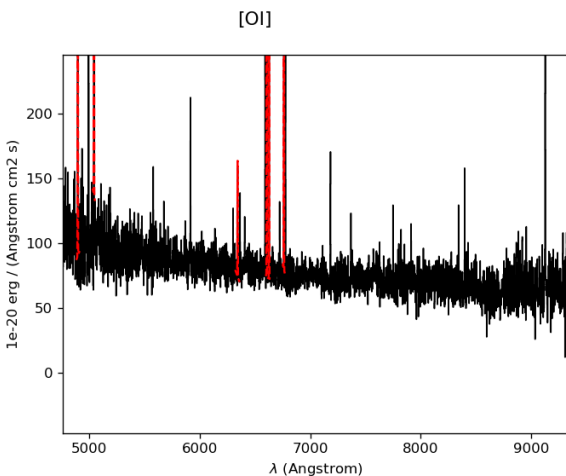
Spectrum of MUSE cube pixel located at the center of the *Swift-XRT* error circle

Spectral fitting



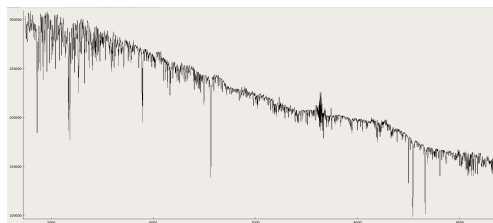
Zoom on the spectral fitting of the $H\alpha$ emission line

Spectral fitting

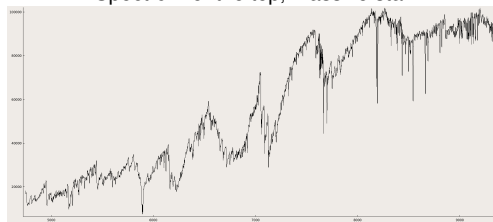


Zoom on the spectral continuum of the MUSE cube pixel located at the center of the center
Swift-XRT error circle

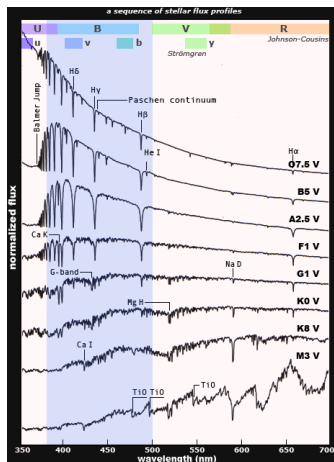
MUSE spectra of the foreground stars



Spectrum of the top, massive star



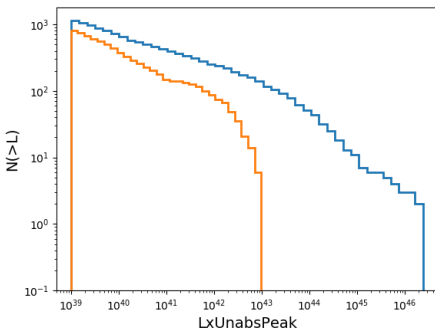
Spectrum of the bottom, low-mass type M star



Reference spectra

<https://www.handprint.com/ASTRO/specclass.html>
master
asep

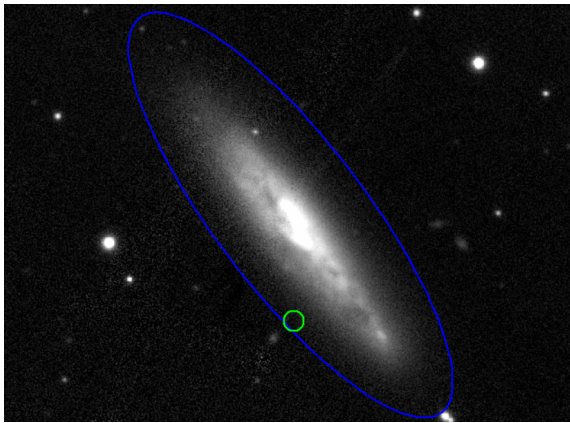
Luminosity Function



Luminosity function of the sources in the ULX/HLX catalog. Blue: total catalog.
Orange: Filtered catalog.

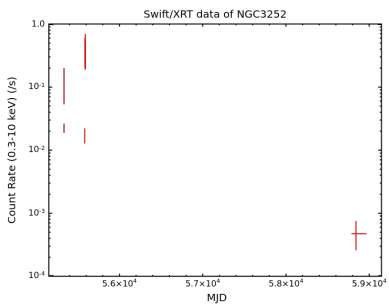
Swartz et al. 2011 showed that the differential ULX luminosity function shows a power law slope $\alpha \propto -1.2$ to -2.0 with an exponential cutoff at $\sim 2 \times 10^{40}$ erg · s⁻¹

NGC 3252

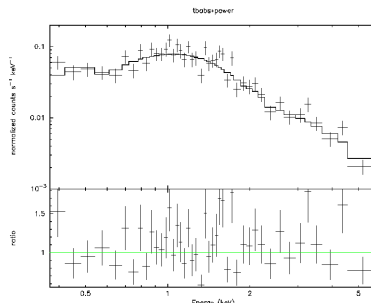


NGC 3252

NGC 3252



Light curve of 2SXPS J103423.1+734519, located in NGC 3252, in the 0.3 – 10 keV band.



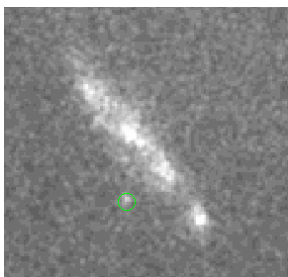
Spectrum of the source using the observations from 2010.

NGC 3252

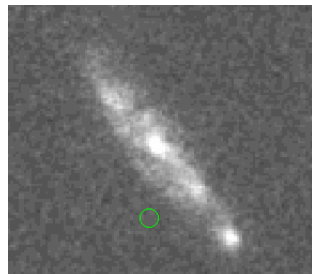
Parameter	Value \pm error (1σ)
N_H	$(1.2^{+0.5}_{-0.4}) \times 10^{21} \text{ cm}^{-2}$
Galactic N_H	$4.6 \times 10^{20} \text{ cm}^{-2}$
Γ	$2.23^{+0.18}_{-0.16}$
Unabsorbed L_X (0.3 – 10 keV)	$1.8 \times 10^{41} \text{ erg} \cdot \text{s}^{-1}$
Peak unabsorbed L_X	$7.1 \times 10^{41} \text{ erg} \cdot \text{s}^{-1}$
χ^2 / dof	48.5/42

Spectral fit parameters using data from 2010

NGC 3252



Swift-UVOT observation of 2SXPS J103423.1+734519 from 2010-2011 in the UVW2 filter.



Swift-UVOT observation from 2019 in the UVW2 filter.

Filter λ (Å)	UVW2	UVM2	UVW1	U	B	V
2010-2011	21.89 ± 0.29	2246	2600	3465	4392	5468
2019	> 22.58	> 21.70	20.52 ± 0.53	20.72 ± 0.16	19.63 ± 0.30	> 19.51

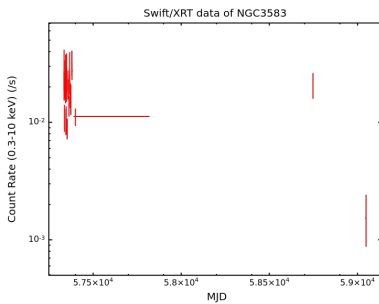
AB magnitudes of the optical counterpart of 2SXPS J103423.1+734519 in different ^{master}*Swift*-UVOT filters, using stacked observations from NGC 3252. Upper limits are computed at 3σ .

NGC 3583

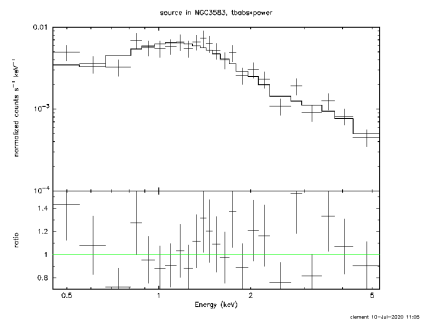


NGC 3583

NGC 3583



Light curve of 2SXPS J111416.1+481833, located in NGC 3583, in the 0.3 – 10 keV band.



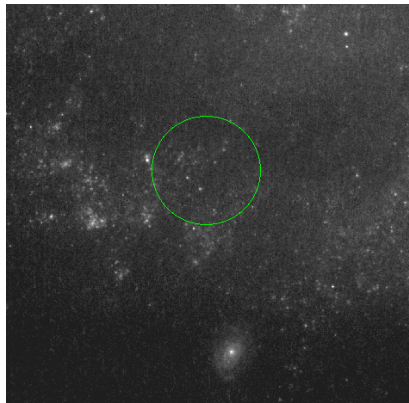
Spectrum of the source using the observations from 2015 and 2020.

NGC 3583

Parameter	Value \pm error (1σ)
N_H	$(1.4^{+0.9}_{-0.8}) \times 10^{21} \text{ cm}^{-2}$
Galactic N_H	$2.4 \times 10^{20} \text{ cm}^{-2}$
Γ	$1.76^{+0.28}_{-0.26}$
Unabsorbed L_X (0.3 – 10 keV)	$(4.4^{+0.5}_{-0.6}) \times 10^{41} \text{ erg} \cdot \text{s}^{-1}$
Peak unabsorbed L_X	$1.7 \times 10^{41} \text{ erg} \cdot \text{s}^{-1}$
χ^2 / dof	18.68/24

Spectral fit parameters using data from 2015 and 2020

NGC 3583



HST image of NGC 3583, in the F814W filter (IR at 8043 Å), taken on 2018-05-14
(exposure time: 1.8 ks)